METAMORPHISM AND GEOTHERMOBAROMETRY OF HIGH-ALUMINA HOOSAC AND PINNEY HOLLOW FORMATION SCHISTS IN THE STAR HILL SIGMOID, CHESTER DOME, VERMONT

James L. Crowley
Geology Dept., Amherst College
Amherst, MA 01002

The Star Hill sigmoid is a domed, isoclinally folded structure consisting of Precambrian and Cambrian schists, gneisses, amphibolites and calc-silicates in the north end of the Chester gneiss dome of southeastern Vermont. The sigmoid is flanked on the east by the axial trace of the Chester dome and on the west by units of the Outer Mantle Sequence in the Proctorsville syncline. As a result of Taconian and Acadian complex recumbent folding and late doming, the rock units in the Star Hill sigmoid have been infolded and isolated by Precambrian gneisses from similar rocks that occur less than one kilometer to the west. The deformational events and subsequent metamorphism in the Star Hill sigmoid are well-documented by Downie (1982). The rocks analyzed in this study are the Hoosac and Pinney Hollow Formation high-alumina schists of probable pre-Taconian affinity that occur as repeating bands in a U-shaped arrangement within the sigmoid (Fig. 1). The Hoosac Formation schists (Unit D in Fig. 1) are lithologically similar, and correlative, with the Gassetts schist studied by A.B. Thompson et al. (1977). The Pinney Hollow schists (Unit A) are at a considerably higher metamorphic grade than similar rocks in the Outer Mantle Sequence. The garnet - staurolite-kyanite isograd lies between the sigmoid and the Outer Mantle Sequence, reflecting the closer position of the sigmoid to the gneisses forming the core of the Chester dome.

The purposes of this project are to: 1.) describe the different continuous and discontinuous metamorphic reactions involved in the formation of the diverse mineral assemblages in the high-alumina schists; 2.) present mineral composition data obtained with an electron microprobe; 3.) elucidate the P-T metamorphic history from different models of geothermobarometry; and 4.) discuss the metamorphism of the Star Hill sigmoid in relation to the Taconian and Acadian orogenies. During August 1988, 160 rock samples were collected, from which 80 thin sections have been prepared for the purpose of petrographic study. Five of these samples were analyzed by a electron microprobe in January 1989, and an additional five are slated for analysis in March.

A variety of textures, inclusion assemblages and mineral composition data document the continuous and discontinuous reactions responsible for the paragenesis of the pelites. These textures include: 1.) chloritized biotite; 2.) chlorite embayment and rimming of garnet; 3.) inclusion-free garnet overgrowth rims; 4.) margarite replacing staurolite; and 5.) both porphyroblastic and deformed kyanite and staurolite. The observed mineral assemblages in the Pinney Hollow and Hoosac Formations suggest that a large portion of the sigmoid was metamorphosed at medium-grade conditions of the staurolite-kyanite zone (Downie, 1982). These assemblages include: garnet+biotite, garnet+biotite+staurolite, garnet+staurolite, garnet+staurolite+chloritoid, garnet+ chloritoid+chlorite, garnet+biotite+staurolite+kyanite, and garnet+staurolite+chlorite (Fig. 4). All of the pelites contain quartz, garnet, muscovite, chlorite, ilmenite, and many also contain plagioclase and paragonite. The presence of four phase AFM assemblages suggests that extra components not accounted for in the KFMASH system (Ca,Mn, Zn) may stabilize one or more additional AFM phases.

The equilibrium assemblages are portrayed in AFM space as a series of metamorphic facies (Fig. 4). There is a consistent change in assemblage across the sigmoid; the southeast and central sections have higher grade assemblages (staurolite and kyanite existing with biotite), and the west and northern sections have lower grade assemblages (staurolite and chloritoid existing without biotite). As shown on the map in figure 1, the higher grade assemblages are found near the core of the Chester dome and the lower grade assemblages occur close to the Outer Mantle Sequence. The isograds denoting this apparent change in grade across the sigmoid parallel Downie's garnet - staurolite-kyanite isograd lying to the west. This diversity in apparent metamorphic grade is explained as a result of different P-T conditions during metamorphism or different bulk compositions of the metasediments. This study attempts to determine which variable was most responsible for the diversity in mineral assemblages.

On the basis of preliminary microprobe data from coexisting minerals, X_{Fe} varies in the order: garnet> staurolite>chloritoid>biotite=chlorite (Fig. 2). Also, the rocks with higher grade assemblages (garnet+biotite+ staurolite+kyanite) contain minerals that have lower X_{Fe} than the minerals in rocks with lower grade assemblages (garnet+biotite+staurolite and garnet+biotite). This variation in X_{Fe} results from tie-line rotation and the migration of three phase triangles across the AFM reaction space toward the A-M sideline with

increasing grade. This movement of tie-lines can be explained through several continuous and discontinuous reactions, such as: 79Kya + 6Chl = 21Sta + 19Qtz + 15H_2O, 116Chl + 237Musc = 90Sta + 79Bio + 183Qtz + 606H_2O, 42Sta + 33Bio + 213Qtz = 116Gar + 99Musc + 42H_2O

During an early metamorphic event the micas and primary chlorite and rolled garnets grew syntectonically, and were succeeded by porphyroblastic staurolite, kyanite, and inclusion-free rims on garnet in a second metamorphic event. Biotite probably grew during both events. This early event is assumed to be the Taconian orogeny and the second event is assumed to be the Acadian orogeny. Unoriented chlorite and chlorite rims on garnet are presumably retrograde and formed during a late cooling event. These schists attained peak metamorphic conditions late in the Acadian. Determining the conditions under which these minerals grew will allow for the characterization of the two orogenies. P-T conditions of metamorphism (Fig. 3) are estimated to have been 7.75 to 8.5 kbar (garnet-biotite-muscovite-plagioclase, Crowley and Hodges, 1985) and 550°C (garnet-biotite, Ferry and Spear, 1978). Additional analysis will provide further insight into apparent grade variation within the sigmoid, additional P-T estimations and paths of metamorphism.

References

Crowley, P.D. and K.V. Hodges, 1985, Error estimation and empirical geothermobarometry for pelitic systems: Am. Mineral., 70, 702-709.

Downie, E.A., 1982, Structure and metamorphism in the Cavendish area, north end of the Chester dome, southeastern Vermont: Ph.D. thesis, Harvard University, MA, 291p.

Ferry, J.M. and F.S. Spear, 1978, Experimental calibration of the partitioning of Fe and Mg between biotite and garnet: Contrib. Mineral Petrol., 66, 113-117.

Thompson, A.B., P.T. Lyttle, and J.B. Thompson, Jr., 1977, Mineral reactions and A-Na-K and AFM facies types in the Gassetts schist, Vermont: Am. Jour. Sci., 277, 1124-1151.

Explanation of Figure 1: Geologic Map of the Star Hill Sigmoid

Unit A: Pinney Hollow Formation
Unit B: Hoosac Formation (low-alumina)
Unit C: Tyson Formation
Unit D: Hoosac Formation (high-alumina, Gassetts schist-like lithology)
Unit E,F,G: Precambrian Mt. Holly Complex

Circles show location of thin section samples. Bold numbers represent samples that have been analyzed with an electron microprobe. Schematic AFM topologies characterize each mineral facies in the general area. Crosses are the observed assemblages, which also contain quartz+muscovite+ilmenite±paragonite±plagioclase. Rock unit locations are from Downie (1982).

Explanation of Figure 3: Preliminary P-T Results From Geothermobarometry

Pressures estimated using garnet-biotite-muscovite-plagioclase geobarometer of Crowley and Hodges (1985).
Temperatures estimated using garnet-biotite geothermometer of Ferry and Spear (1978).
Numbers indicate probed samples.

Explanation of Figure 4: AFM Mineral Facies

Schamtic AFM topologies characterizing each mineral facies. Crosses represent observed mineral facies. All assemblages shown contain quartz + muscovite + ilmenite ± plagioclase ± paragonite.

Fig. 1: Geologic Map of the Star Hill Sigmoid

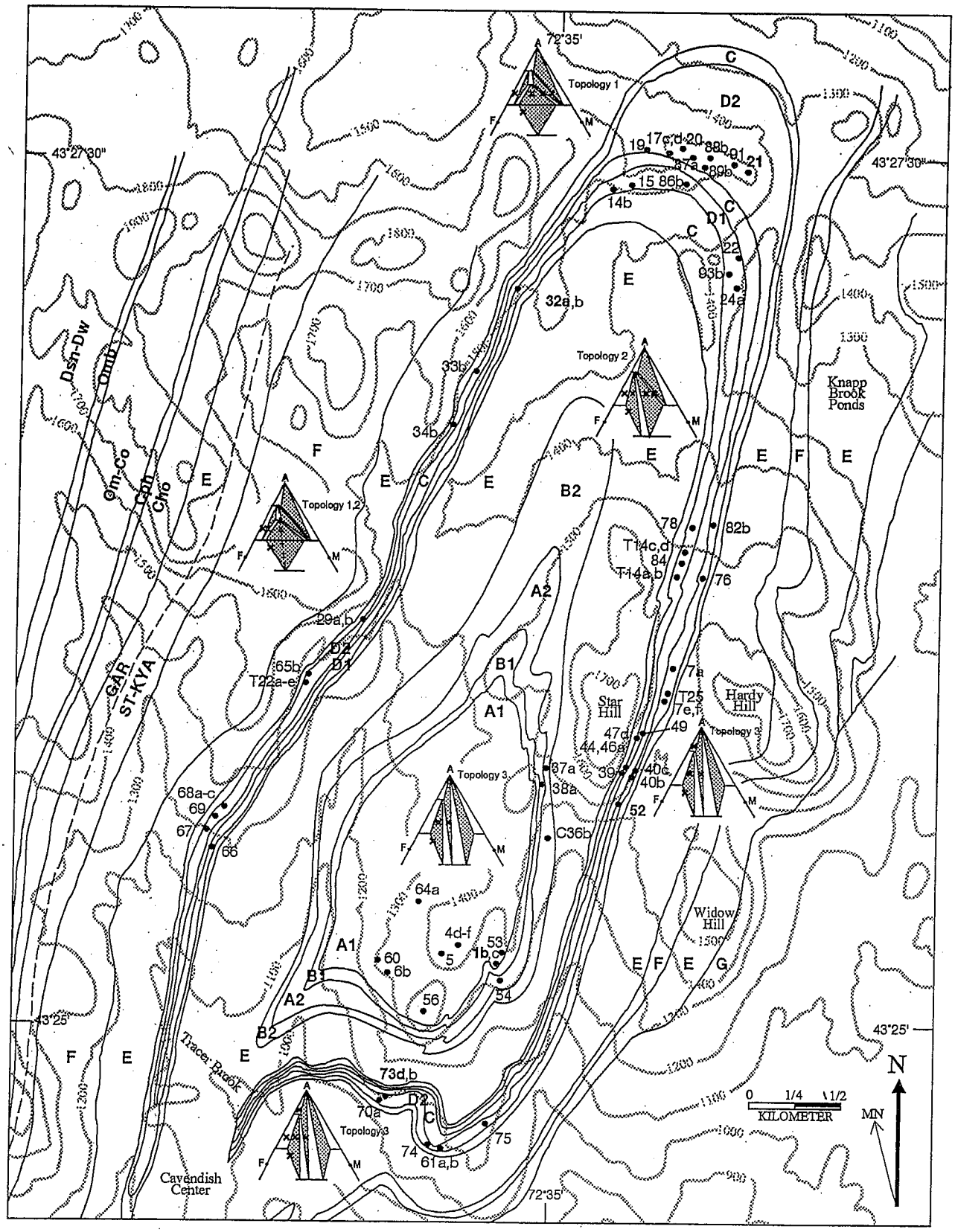

Fig.2: Compiled AFM Projections-Compositions from Probe Data

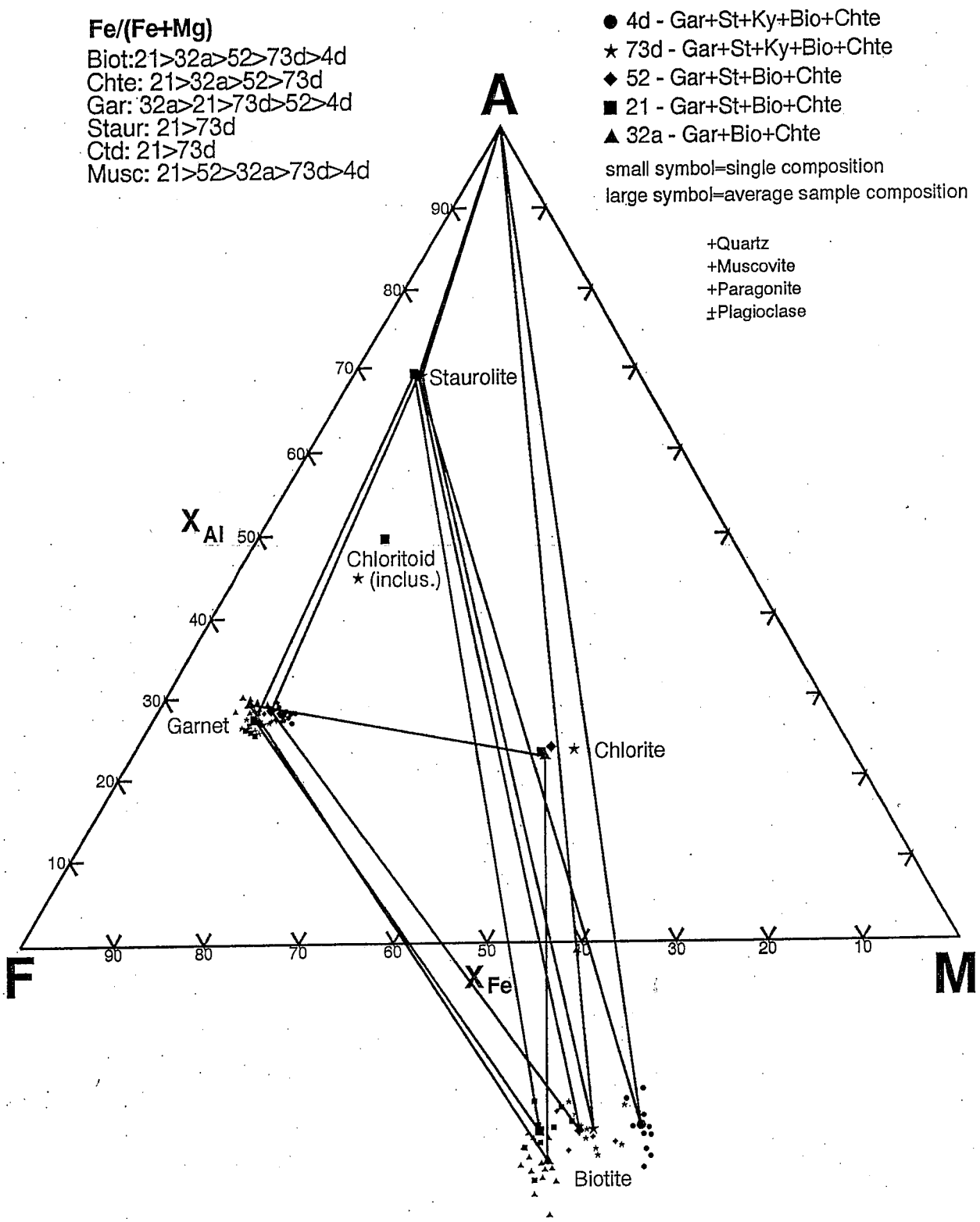

Fig. 3: Preliminary P-T Results From Geothermobarometry

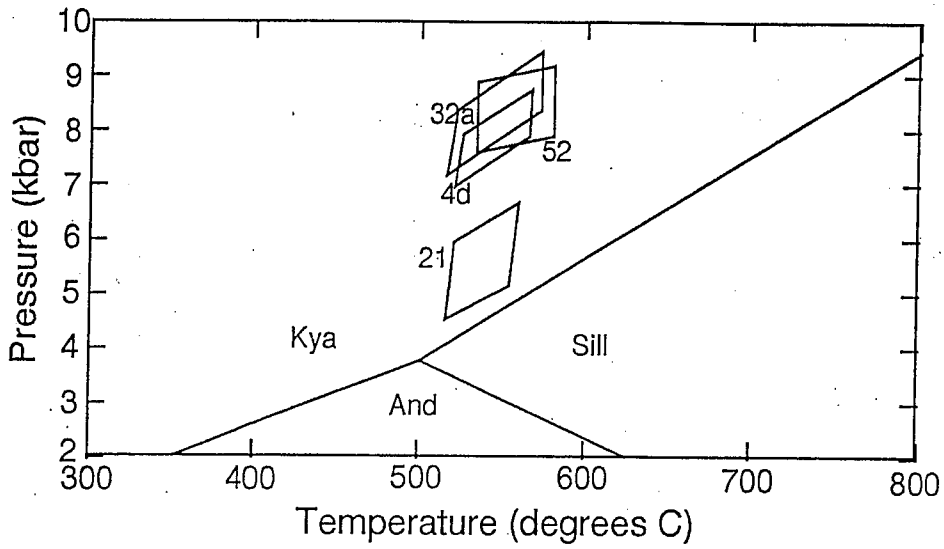

Fig. 4: AFM Mineral Facies